Condition for the appearance of the metastable $P_{\beta'}$ phase in fully hydrated phosphatidylcholines as studied by small-angle x-ray diffraction

Sinzi Matuoka,* Haruhiko Yao,‡ Satoru Kato§ and Ichiro Hatta||

*Department of Physics, Sapporo Medical College, S.1, W.17, Chuo-ku, Sapporo 060, Japan; ‡Department of Physics, Tokyo Institute of Technology, Tokyo 152, Japan; §Department of Physics, Kwansei Gakuin University, Nishinomiya 662, Japan; ||Department of Applied Physics, Nagoya University, Nagoya 464-01, Japan.

ABSTRACT In the ripple phase of fully hydrated multilamellar vesicles of dipalmitoylphosphatidylcholine (DPPC), two kinds of small-angle x-ray diffraction profiles are observed on cooling through the main transition. One is a seemingly normal profile similar to that observed on heating and the other is the superposition of the diffraction profiles for the primary (normal) and the secondary ripple structures. We found that the profile obtained depended on the cooling rate. Increasing the cooling rate from 0.1°C/min to 1°C/min caused the peaks originating from the secondary ripple structure to diminish. After a cooling scan at 43°C/min, the profile became similar to that of the normal ripple structure, although a trace of the secondary ripple structure remains. The results are interpreted in terms of the rise and fall of three-dimensional correlated domains composed of both primary and secondary ripple structures. At slow cooling rates, correlated domains of both kinds of ripple structures develop. As the cooling rate is increased, the domain of the primary ripple structure remains correlated, while that of the secondary ripple structure becomes less correlated. In addition, the multipeak profile appears even at rapid cooling rates, if the final low temperature lies just below the T_m for the main transition. This results suggests that formation of the correlated domains of the secondary ripple structure requires a certain time interval during which the DPPC vesicles experience the temperature just below the main transition. The secondary ripple structure takes place in phosphatidylcholines having more than 15 carbons in each hydrocarbon chain upon cooling through the main transition.

INTRODUCTION

The metastable $P_{\beta'}$ phase ($P_{\beta'}$(mst)) of fully hydrated dipalmitoylphosphatidylcholine (DPPC), first reported by Tenchov et al. (1), is characterized by its complex multipeak x-ray diffraction profile in low angle region from 3 nm to 10 nm. This new phase takes place when DPPC is cooled at a slow rate (0.1–0.5°C/min) through the main transition, and its x-ray diffraction profile is quite different from that of the normal $P_{\beta'}$ phase appearing in heating run, which has been reported (2–4). Tenchov et al. (1) have concluded that the phase appearing in the cooling run is metastable because the transition enthalpy from the $P_{\beta'}$ (mst) phase to the L_α phase was about 5% less than that from the normal $P_{\beta'}$ phase to the L_α phase.

Yao et al. (5) have explained the complex x-ray diffraction peaks in terms of the coexistence of both primary and secondary ripple structures. These ripple structures had been reported in experiments of freeze-fracture electron microscopy (6–9), where the primary and the secondary ripple wavelengths are about 14 and 25 nm, respectively. Yao et al. (5) have observed the x-ray diffraction peak at 26.4 nm, giving clear evidence for the appearance of the secondary ripple structure in slow cooling. These results suggest that the metastability of the new ripple phase is related to the formation of the secondary ripple structure. In the present paper we restate that the primary and the secondary ripple structures are those for the $P_{\beta'}$ phase and the metastable $P_{\beta'}$ phase ($P_{\beta'}$(mst)), respectively. In this sense the complex multipeak profile reflects the coexistence of the $P_{\beta'}$(mst) phase and the $P_{\beta'}$ phase.

In contrast, Caffrey et al. (10) have pointed out no significant difference in small-angle x-ray diffraction profiles between the ripple phases produced in heating or cooling. They have assumed that lack of the multipeak x-ray diffraction profile is caused by a difference of cooling rate through the main transition, i.e., the rapid cooling rate of 2.8°C/s (168°C/min) in Caffrey et al. and the slow rate of 0.1°C/min in Tenchov et al. (1), or the result of differences of the solutions (Caffrey used Hepes/NaCl/KCl buffer, while Tenchov et al. used deionized water).

In this paper, we will clarify the condition for the appearance of the multipeak x-ray diffraction profile in connection with the formation of the secondary ripple structure (the $P_{\beta'}$(mst) phase).

MATERIALS AND METHODS

1,2-distearoyl-*sn*-glycero-3-phosphocholine (DSPC), 1,2-dipalmitoyl-*sn*-glycero-3-phosphocholine (DPPC), 1,2-dipentadecanoyl-*sn*-glycero-3-phosphocholine (C15PC), 1,2-dimyristoyl-*sn*-glycero-3-phosphocholine (DMPC) and 1,2-ditridecanoyl-*sn*-glycero-3-phosphocholine (C13PC) were purchased from Avanti Polar Lipids Inc. (Birmingham, AL, USA). Multilamellar vesicles of these lipids were prepared as previously reported (11). Distilled water was used for hydration; buffer solution was not used. The water content was in the

Address correspondence to Dr. Sinzi Matuoka, Department of Physics, Sapporo Medical College, S.1, W.17, Chuo-ku, Sapporo 060, Japan.

0006-3495/93/05/1456/05 $2.00

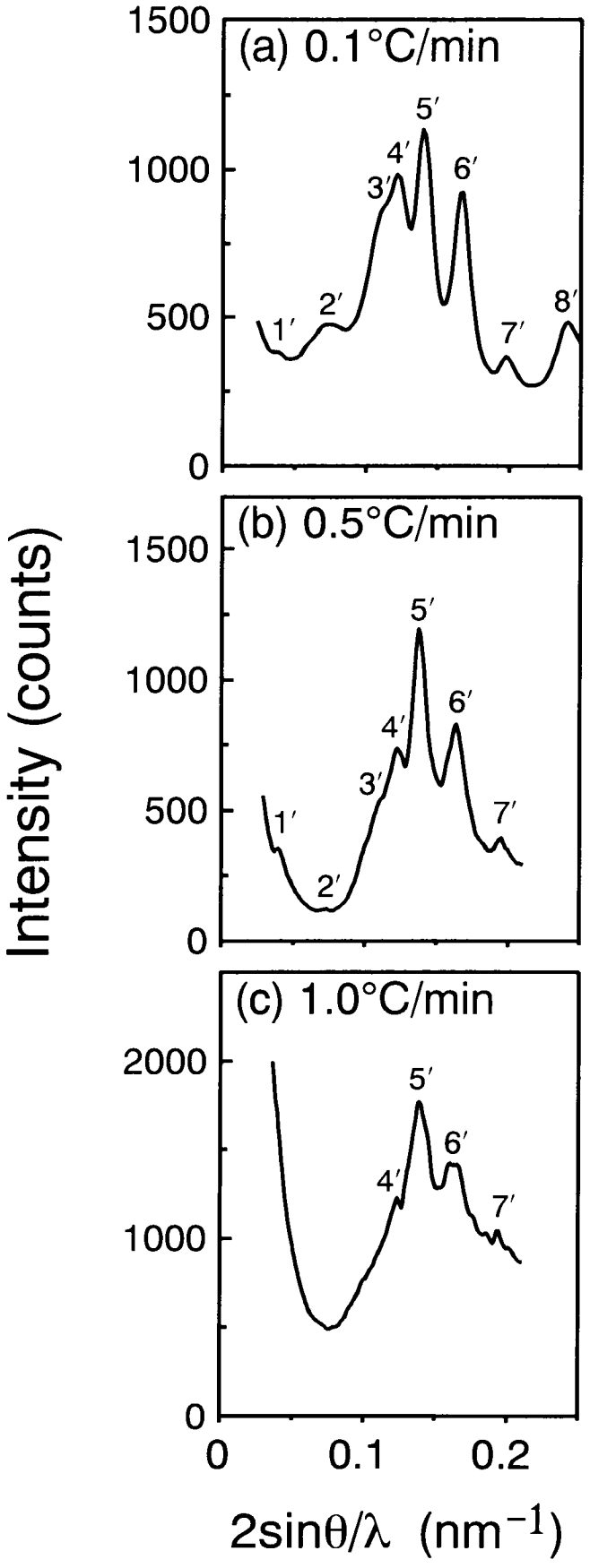

range of 55 wt% to 65 wt%, which corresponds to an excess water condition.

Small-angle x-ray diffraction measurements using synchrotron radiation were carried out using a monochromatic x-ray beam (λ = 0.150 nm) at the BL-15A Station of the Photon Factory, National Laboratory for High Energy Physics, in Tsukuba, Japan. The design of the small-angle x-ray diffractometer has been described in detail (12). Diffracted x-rays were detected with a one-dimensional position-sensitive proportional counter (Rigaku, Tokyo, Japan) of which channel-to-channel distance was 0.368 mm. The sample-to-detector distance measured by a ruler was 2,534.5, 2,525, 1,226.5, and 1,035 mm. The resolution for the scattering angles ($\Delta 2\theta$) were 0.008°, 0.008°, 0.017°, and 0.020°, which correspond to a resolution for the spacing of 0.05, 0.05, 0.10, and 0.11 nm at a spacing of 7 nm, respectively. The uncertainty in the spacing arising from error in sample-to-detector distances is within these resolutions. For recording the profiles of the $P_{\beta'}$(mst) the sampling time reached to 420–780 s to get a sufficient signal-to-noise ratio.

The sample was set in the hole of an aluminum plate and was sealed by mylar sheets at both sides. This plate containing the sample was immersed in a water jacket in which water flows (13 liters/min) from a temperature-controlled water bath (model RCS-20D; Messgeräte-werk Lauda, Germany) as described previously (1, 11). The temperature of the sample was monitored with a chromel–alumel thermocouple attached to the plate. Thermoelectromotive force of the thermocouple was detected with a digital multimeter (model 195A; Keithley Instruments, Inc., Cleveland, OH, USA) and stored by a personal computer (model PC9801F; NEC Corp., Tokyo, Japan) at 6 s intervals. Rapid cooling experiments were performed by switching one water flow at an initial temperature to another at the final temperature by using electric valves (CKD Co., Japan). On rapid cooling from 43°C to 38°C the cooling rate at the main transition temperature was about 43°C/min. Temperature overshoot during rapid cooling was less than 0.1°C.

RESULTS AND DISCUSSION

When fully hydrated DPPC is slowly cooled through the main transition, the multipeak x-ray diffraction profile appears as reported in the previous works by Tenchov et al. (1) or by Yao et al. (5). The profile obtained after a cooling scan at 0.1°C/min through the main transition is drawn in Fig. 1 *a*. Peaks 3′, 4′, 6′, and 7′ clearly appear; these correspond to the (03), (10) for the secondary ripple structure ($P_{\beta'}$(mst)), (11) and (1–2) for the primary ripple structure ($P_{\beta'}$), respectively (see Table 1). However, after cooling at a faster rate of 0.5°C/min, peak no. 3′ appears only as a shoulder and the intensity of the peaks nos. 4′, 6′, and 7′ decrease (see Fig. 1 *b*). At a faster cooling rate of 1.0°C/min peak no. 3′ disappears and the intensities of the peaks nos. 4′ and 6′ are reduced considerably as seen in Fig. 1 *c*.

The x-ray diffraction profile at 38°C of fully hydrated DPPC after rapid cooling (~43°C/min) through the main transition is displayed in Fig. 2 (thick line). This

FIGURE 1 X-ray diffraction profiles of fully hydrated DPPC obtained after slow cooling at rates of *a*) 0.1°C/min, *b*) 0.5°C/min, and *c*) 1.0°C/min. Final temperatures of the samples were 40°C in *a*) and 37.8°C in *b*) and *c*). Sampling times were 780 s, 420 s, and 600 s in *a*), *b*), and *c*), respectively. Sample-to-detector lengths were 1,226.5 mm in *a*), and 2,525 mm in *b*) and *c*). For the peaks denoted by no. 1′ to no. 8′ see Table 1.

TABLE 1 **Indexing in the two-dimensional monoclinic unit cell (*hk*) for the diffraction profiles in the ripple phase (the $P_{\beta'}$ phase or the $P_{\beta'}$(mst) phase) of fully hydrated DPPC near 38°C**

a)

Peak no.	d_{obs} (nm)	Primary ripple structure d_{cal} (nm) (*hk*)	Secondary ripple structure d_{cal} (nm) (*hk*)
1′	25.4 ± 0.6		— (01)
2′	13.6 ± 0.2	13.2 (01)	
3′	~9		
4′	8.19 ± 0.07		— (10)
5′	7.29 ± 0.05	7.29 (10)	
6′	6.13 ± 0.04	6.13 (11)	
7′	5.13 ± 0.03	5.13 (1–2)	

b)

Peak no.	d_{obs} (nm)	Primary ripple structure d_{cal} (nm) (*hk*)
1	13.8 ± 0.5	13.4 (01)
2	7.45 ± 0.13	7.45 (10)
3	6.19 ± 0.09	6.19 (11)

c)

Peak no.	d_{obs} (nm)	Primary ripple structure d_{cal} (nm) (*hk*)
1	13.8 ± 0.5	13.6 (01)
2	7.21 ± 0.12	7.21 (10)
3	6.27 ± 0.09	6.27 (11)

Peak nos. in *a*), *b*), and *c*) correspond to those of Fig. 1 *b*, Fig. 2 (*thick line*), and Fig. 2 (*thin line*), respectively. The spacings d_{obs} are the observed spacings and d_{cal} denote the calculated ones from the following lattice parameters: a = 7.32 nm, b = 13.21 nm, and γ = 95.5° in *a*); a = 7.51 nm, b = 13.55 nm, and γ = 97.3° in *b*); a = 7.22 nm, b = 13.60 nm, and γ = 92.3° in *c*). Only indexing (*hk*) for the secondary ripple structure is listed in *a*) because d_{cal} cannot be calculated from two observed peaks.

profile is similar to that obtained in the heating run (Fig. 2, thin line). This result is consistent with that by Caffrey et al., although they used lipid dispersed in HEPES/NaCl/KCl buffer and microwave radiation for heating. Thus, it is obvious that a key factor for appearance of the multipeak profile is the cooling rate.

However, even on rapid cooling (11°C/min) a multipeak diffraction profile was obtained as seen in the Fig. 3 *a*, where DPPC was cooled down to 41.0°C, just below the main transition temperature of 41.37°C (1). This profile is very similar to those obtained after slow cooling through the main transition at a rate of 0.1°C/min (Fig. 1 *a*) rather than that at 41.0°C on heating (see Fig. 3 *b*) or on rapid cooling to 37.8°C (Fig. 2, thick line). Thus we conclude that the crucial factor for the formation of a multipeak profile is not the cooling rate, but the time interval during which DPPC multibilayers are kept just below the main transition temperature. The dependence of the profiles on scanning rate is explained in terms of this "staying time" just below the main transition, i.e., the staying time becomes longer with slower cooling rate. Thus the multipeak profile is realized in both slow cooling experiments and rapid cooling experiments, to a temperature just below the main transition.

In Fig. 2, the appearance of the sharp (10) reflection on rapid cooling and on heating indicates formation of the primary ripple structure in both cases. However, the x-ray intensities diffracted in the range from 0.08 nm^{-1} to 0.3 nm^{-1} (except around the (10) peak region) are rather higher on rapid cooling than on heating as seen in Fig. 2. The difference between them suggests the existence of broad reflections around 4.0, 5.3, and near 9 nm on rapid cooling. These reflect peaks which are characteristic of the multipeak profile; the (20) peak for the secondary ripple structure, the (1–3) peak for the primary one and the (03) peak for the secondary one, respectively (5). Therefore, the existence of the broad reflection indicates formation of the secondary ripple structure.

In addition, recent freeze-fracture electron microscopy experiments (Kato, S., K. Miyazawa, H. Miyamoto, K. Honda, and I. Hatta, submitted for publication) show that secondary ripple structure is formed even in the rapid cooling experiments. Thus we conclude that the formation of the $P_{\beta'}$(mst) phase takes place whenever DPPC is cooled from the L_α phase irrespective of cooling rate.

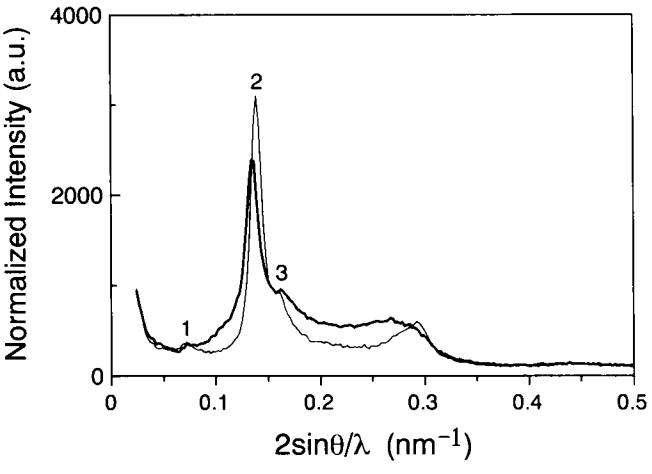

FIGURE 2 X-ray diffraction profiles in the ripple phase (the $P_{\beta'}$ phase or the $P_{\beta'}$ (mst) phase) of fully hydrated DPPC. These are obtained after rapid cooling from 43°C to 38.0°C at a cooling rate of 43°C/min (*thick line*) or 38.0°C in heating run (*thin line*). Sampling times were 180 s. Sample-to-detector lengths were 1,035 mm. The intensity scales for both profiles are normalized with an incident x-ray intensity monitored by an ion chamber current detected in front of the sample. For the peaks denoted by no. 1 to no. 3, see Table 1.

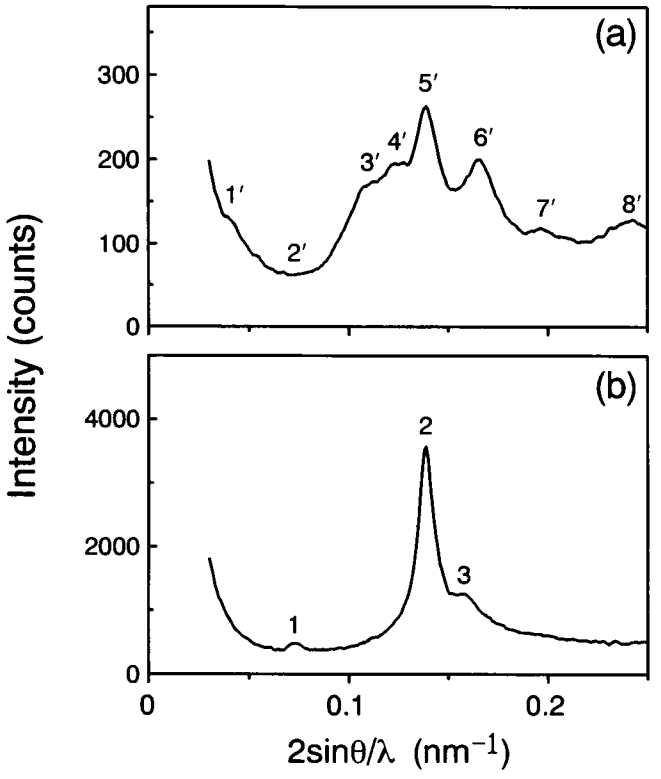

FIGURE 3 X-ray diffraction profiles in the ripple phase (the $P_{\beta'}$ phase or the $P_{\beta'}$ (mst) phase) of fully hydrated DPPC obtained *a*) after rapid cooling from 42°C to 41.0°C (cooling rate of 11°C/min), and *b*) at 41.0°C in heating run. Sampling times were 780 s in *a*) and 300 s in *b*). Sample-to-detector lengths were 2,534.5 mm. For the peaks denoted by no. 1′ to no. 8′ and no. 1 to no. 3, see Table 2.

Why does the multipeak profile fade away on rapid cooling as in Fig. 2 in spite of the formation of the $P_{\beta'}$(mst)? After cooling through the main transition, at least three kinds of domains may be generated, that is, three-dimensional correlated domains of the primary ripple structure, three-dimensional correlated ones of the secondary ripple structure, and uncorrelated regions. Among these domains, three-dimensional correlated domains result in sharp x-ray diffraction peaks. Thus we interpret the lack of the multipeak profile in terms of the rise and fall of these correlated domains of the primary and secondary ripple structures. When DPPC is slowly cooled through the main transition, both correlated domains of the primary and secondary ripple structures develop and generate the multipeak profile. In contrast, upon rapid cooling (except for rapid cooling to 41°C) the correlated domains of the primary ripple structure develop, but secondary ripple structure does not show distinct correlated domains.

From the above results, we speculate on the formation process of the primary and the secondary ripple structures. When DPPC multilamellar vesicles are cooled through the main transition, nuclei of both secondary and primary ripple structures are formed. The domain of the primary ripple structure may be correlated rapidly. On the other hand, the formation of the correlated domain of the secondary ripple structure requires that DPPC multilamellar vesicles experience the temperature just below the main transition for a certain time interval.

Indices and lattice parameters in DPPC at 41.0°C for Fig. 3 are summarized in Table 2. The peak no. 3′ was indexed to '(03)' of the secondary ripple structure in our previous indexing (5). However, the spacing of peak no. 3′ seems to significantly deviate from one-third of the (01) spacing of the secondary ripple peak, no. 1′, and furthermore its intensity is rather high compared to results showing that the intensity of the (03) peak is smaller than that of the (01) peak (13). Thus, this assignment is not conclusive at present. Since the corresponding peak intensity develops upon slow cooling at 0.1°C/min or on rapid cooling to a temperature just below the main transition (Fig. 3 *a*), this peak might be due to mismatch between the secondary ripple plane and the primary ripple plane.

The formation of the $P_{\beta'}$(mst) phase, that is, the appearance of the secondary ripple structure, depends on hydrocarbon chain length. In ditridecanoylphosphatidylcholine (C13PC) and dimyristoylphosphatidylcho-

TABLE 2 **Indexing in the two-dimensional monoclinic unit cell (*hk*) for the diffraction profiles in the ripple phase (the $P_{\beta'}$ phase or the $P_{\beta'}$(mst) phase) of fully hydrated DPPC at 41°C**

a)

Peak no.	d_{obs} (nm)	Primary ripple structure d_{cal} (nm) (*hk*)	Secondary ripple structure d_{cal} (nm) (*hk*)
1′	25.2 ± 0.6		26.2 (01)
2′	—	12.9 (01)	
3′	9.17 ± 0.08		
4′	8.2 ± 0.07		8.20 (10)
5′	7.22 ± 0.05	7.22 (10)	
6′	6.02 ± 0.04	6.02 (11)	
7′	5.10 ± 0.03	5.10 (1–2)	
8′	4.11 ± 0.02		4.10 (20)

b)

Peak no.	d_{obs} (nm)	Primary ripple structure d_{cal} (nm) (*hk*)
1	13.4 ± 0.2	13.4 (01)
2	7.23 ± 0.05	7.23 (10)
3	6.3 ± 0.04	6.30 (11)

Peak nos. in *a*) and *b*) correspond to those of Figs. 3 *a*) and 3 *b*), respectively. The spacings d_{obs} are the observed spacings and d_{cal} denote the calculated spacings from the following lattice parameters: a = 7.27 nm, b = 12.97 nm, and γ = 96.4° for the primary ripple structure in *a*); a = 8.21 nm, b = 26.25 nm, and γ = 87.3° for the secondary ripple structure in *a*); a = 7.23 nm, b = 13.43 nm, and γ = 91.4° in *b*).

line (DMPC) the profiles obtained after slow cooling through the main transition agree with that for a normal $P_{\beta'}$ phase, while the secondary ripple structure appears in C15PC, DPPC, and DSPC. Thus, we conclude that the secondary ripple structure in PCs having more than 15 carbons in a hydrocarbon chain is generated whenever these PCs are cooled through the main transition, irrespective of the cooling rate.

We are grateful to Prof. M. Akiyama and Prof. K. Ohki for useful discussions, and to Dr. Y. Amemiya for helpful advice on the instrumentation of synchrotron x-ray small-angle experiments.

This work is supported in part by a Grant-in-Aid for General Scientific Research from the Ministry of Education, Science and Culture, Japan.

Received for publication 27 January 1992 and in final form 15 December 1992.

REFERENCES

1. Tenchov, B. G., H. Yao, and I. Hatta. 1989. Time-resolved x-ray diffraction and calorimetric studies at low scan rates I. Fully hydrated dipalmitoylphosphatidylcholine (DPPC) and DPPC/water/ethanol phases. *Biophys. J.* 56:757–768.
2. Tardieu, A., V. Luzzati, and F. C. Reman. 1973. Structure and polymorphism of the hydrocarbon chains of lipids: a study of lecithin-water phases. *J. Mol. Biol.* 75:711–733.
3. Janiak, M. J., D. M. Small, and G. G. Shipley. 1976. Nature of the thermal pretransition of synthetic phospholipids: dimyristoyl- and dipalmitoyllecithin. *Biochemistry.* 15:4575–4580.
4. Stamatoff, J., B. Feuer, H. J. Guggenheim, G. Tellez, and T. Yamane. 1982. Amplitude of rippling in the P_β phase of dipalmitoyl-phosphatidylcholine bilayers. *Biophys. J.* 38:217–226.
5. Yao, H., S. Matuoka, B. G. Tenchov, and I. Hatta. 1991. Metastable ripple phase of fully hydrated dipalmitoyl-phophatidylcholine as studied by small angle x-ray scattering. *Biophys. J.* 59:252–255.
6. Copeland, B. R., and H. M. McConnell. 1980. The rippled structure in bilayer membranes of phosphatidylcholine and binary mixtures of phosphatidylcholine and cholesterol. *Biochim. Biophys. Acta.* 599:95–109.
7. Rüppel, D., and E. Sackmann. 1983. On defect in different phases of two-dimensional lipid bilayers. *J. Phys. (Paris).* 44:1025–1034.
8. Zasadzinski, J. A. N., and Schneider, M. B. 1987. Ripple wavelength, amplitude, and configuration in lyotropic liquid crystals as a function of effective headgroup size. *J. Phys. (Paris).* 48:2001–2011.
9. Hicks, A., M. Dinda, and M. A. Singer. 1987. The ripple phase of phosphatidylcholines: effect of chain length and cholesterol. *Biochim. Biophys. Acta.* 903:177–185.
10. Caffrey, M., G. Fanger, R. L. Magin, and J. Zhang. 1990. Kinetics of the premelting ($L_{\beta'}$–$P_{\beta'}$) and main transition ($P_{\beta'}$–L_α) in hydrated dipalmitoylphosphatidylcholine. A time-resolved x-ray diffraction study using microwave-induced temperature-jumps. *Biophys. J.* 58:677–686.
11. Matuoka, S., S. Kato, M. Akiyama, Y. Amemiya, and I. Hatta. 1990. Temperature dependence of the ripple structure in dimyristoylphosphatidylcholine studied by synchrotron x-ray small-angle diffraction. *Biochim. Biophys. Acta.* 1028:103–109.
12. Amemiya, Y., K. Wakabayashi, T. Hamanaka, T. Wakabayashi, T. Matsushita, and H. Hashizume. 1983. Design of a small-angle X-ray diffractometer using synchrotron radiation at the photon factory. *Nucl. Instrum. Methods.* 208:471–477.
13. Wack, D. C., and W. W. Webb. 1989. Synchrotron x-ray study of the modulated lamellar phase $P_{\beta'}$ in the lecithin-water system. *Phys. Rev. A.* 40:2712–2730.